processes

MDPI

Article

Preparation and Mechanism of EP-HMTA-SiO_2 Nanocomposite Polymer Gel for Enhancing Oil Recovery

Weiyou Zhang [1,*], Yongpeng Sun [2], Xianghua Meng [1] and Rutong Dou [1]

[1] College of Energy and Mechanical Engineering, Dezhou University, Dezhou 253023, China; mengxianghuadz@163.com (X.M.); dourutong@163.com (R.D.)
[2] School of Petroleum Engineering, China University of Petroleum (East China), Qingdao 266580, China; sunyongpeng@upc.edu.cn
* Correspondence: zhangweiyou111@163.com

Abstract: During oilfield production, organic substances such as asphaltenes and resins present in crude oil are prone to adsorb onto the surfaces of reservoir rocks. This adsorption process can lead to the conversion of hydrophilic rock surfaces into more oleophilic interfaces, which in turn reduces the permeability and porosity of the reservoir, ultimately affecting the overall recovery efficiency. Consequently, targeted modification of reservoir wettability presents a promising strategy for enhancing recovery rates. In this study, a polymer layer comprising large molecular side chains and hydroxyl groups was synthesized on the surface of nano-SiO_2 to enhance the thermal stability of the polymer. Additionally, the hydroxyl groups were employed to improve the wettability of the core material and reduce interfacial tension. The polymers were characterized using techniques such as FTIR and TG, and the results revealed that the modified SiO_2 exhibited superior performance in reducing both interfacial tension and contact angle when compared to the SiO_2. Injection of a 0.4 wt% EP-HMTA-SiO_2 solution resulted in an increase in recovery rates by 16.4% and 13.2% in medium- and low-permeability cores, respectively.

Keywords: modified nano-SiO_2; polymers; enhanced oil recovery; interfacial tension; contact angle

check for updates

Academic Editors: Zhijie Wen and Jian Tao

Received: 21 January 2025
Revised: 12 February 2025
Accepted: 15 February 2025
Published: 20 February 2025

Citation: Zhang, W.; Sun, Y.; Meng, X.; Dou, R. Preparation and Mechanism of EP-HMTA-SiO_2 Nanocomposite Polymer Gel for Enhancing Oil Recovery. *Processes* **2025**, *13*, 596. https://doi.org/10.3390/pr13030596

Copyright: © 2025 by the authors. Licensee MDPI, Basel, Switzerland. This article is an open access article distributed under the terms and conditions of the Creative Commons Attribution (CC BY) license (https://creativecommons.org/licenses/by/4.0/).

1. Introduction

In recent years, while green energy sources have partially mitigated energy consumption, oil remains the primary energy source for human society [1,2]. As a result, the exploration and development of unconventional oil reservoirs have become an inevitable trend. Medium- and low-permeability oil reservoirs are one such category of unconventional resources. These reservoirs are widely distributed across China, accounting for approximately 50% of all proven oil reserves, with oil and gas reserves comprising about 70% of the total proven reserves, representing a significant economic value [3,4]. However, these reservoirs are characterized by low permeability (1–50 mD), small pore throat sizes, high specific surface area, and severe heterogeneity [5,6]. As a consequence, researchers have focused on waterflooding and chemical enhanced oil recovery (EOR) techniques to improve recovery rates for such reservoirs.

The severe heterogeneity of these reservoirs leads to issues during gas or water flooding, where flow may bypass low-permeability zones, forming channels only in high-permeability areas, resulting in the phenomenon of "fingering". This causes significant amounts of residual oil in low-permeability zones that remain unrecovered. It is estimated that conventional recovery methods, such as gas and water flooding, may leave 60–70%

of the oil behind in the reservoir [7–9]. Polymer flooding is a mature and widely used technique for improving recovery in medium- to high-permeability reservoirs [10–12]. Compared to water flooding, polymer flooding can improve the injectivity of the fluid by increasing the viscosity of the water phase. This enhances the mobility, plugging, and re-mobilization properties of the injected fluid, improves the flow paths of water in heterogeneous reservoirs, and helps mobilize residual oil, thereby increasing the swept volume and overall recovery [13].

Due to the small pore throat sizes and complex flow paths in medium- and low-permeability reservoirs, polymer solutions are prone to shear degradation, leading to a significant reduction in viscosity during the flooding process [14,15]. As a result, researchers have found that adding specific nanoparticles to polymer solutions or grafting nanoparticles onto polymer chains can significantly improve recovery efficiency. Polymer-nanoparticle composites have thus emerged as a promising solution for addressing residual oil in reservoirs [16,17]. For example, Xie et al. [18] analyzed the role of HPAM in enhancing oil recovery, concluding that its main function is to transport oil, with this transport effect being linked to the viscoelastic properties of high molecular weight anionic polyacrylamide (HPAM) solutions, finding that the better the viscoelasticity, the higher the oil recovery efficiency. Cheng et al. [19] grafted SiO_2 nanoparticles onto polyacrylamide/2-acrylamido-2-methylpropanesulfonic acid sodium salt, and through electron microscopy and core flooding experiments, they observed the presence of macromolecular chains on the surface of SiO_2 nanoparticles, which contributed to the improved oil recovery performance. Yao et al. [20] studied the migration and plugging mechanisms of HPAM polymer in pore channels using a transparent quartz sand-packed model. The results indicated that the colloidal and hydrodynamic forces jointly control the deposition and release of the polymer on the surface of porous media. The polymer molecules, through mechanisms such as capture, accumulation, and bridging, block small pore throats, leading to increased pressure in the blocked throats, which facilitates the mobilization of oil from adjacent pores or throats, thereby enhancing the swept volume and recovery.

In this study, a modified SiO_2-grafted polyacrylamide hyperbranched copolymer was synthesized to enhance oil recovery in medium- and low-permeability reservoirs. Through a two-step grafting process, the copolymer incorporated functional groups that significantly improved the material's performance. Compared to unmodified SiO_2, the modified polymer exhibited increased molecular side chains and a high density of hydroxyl groups, resulting in enhanced steric hindrance. This structural modification improved both the thermal stability and viscosity of the polymer solution. The increased viscosity plays a crucial role in the enhanced oil recovery (EOR) process. It helps reduce interfacial tension and contact angle, two key factors in facilitating oil displacement. In addition, the higher viscosity of the polymer solution leads to a reduced water–oil mobility ratio, which improves the sweep volume and overall displacement efficiency. Experimental results showed that the injection of a 0.4 wt% SiO_2-grafted polyacrylamide hyperbranched copolymer led to a 16.4% increase in recovery in medium-permeability cores and a 13.2% increase in low-permeability cores. These improvements are attributed to the combined effects of enhanced viscosity, optimized wettability, and better flow control within the reservoir. Overall, the modified SiO_2-grafted polyacrylamide hyperbranched copolymer proves effective in improving recovery efficiency, particularly in challenging medium- and low-permeability reservoirs. The results highlight the potential of this modified polymer for enhancing oil recovery by addressing key factors such as interfacial tension, wettability, and fluid mobility.

2. Materials and Methods

2.1. Materials

The nano-SiO_2 was provided by BowsNano Technology Co., Ltd. (No. 5 Yinxiang Road, Dongjiao Industrial Park, Yuyao, China) γ-Methacryloxypropyltrimethoxysilane (KH570), 4-ethenylphenol (EP), and dichlorobenzene were supplied by Aladdin Reagent Co., Ltd. (No. 809 Chuhua Branch Road, Shanghai, China) Hexamethylenetetramine (HMTA) was provided by China National Pharmaceutical Group Corp. (No. 200 Newton Road, Zhangjiang Town, Shanghai, China) Reagents used in the study were of analytical grade and did not require further purification. Crude oil and simulated formation water (mineralization degree is 30,000 ppm) were provided by the Southwest Petroleum Branch of PetroChina Natural Gas Research Institute (No. 218 Tianyan Road, Chengdu, China).

2.2. The Preparation of EP-HMTA-SiO_2

The EP-HMTA-SiO_2 composite was synthesized through a two-stage process, as outlined in Figure 1. In the first stage, KH570-modified SiO_2 (KH570-SiO_2) was prepared. In a 500 mL beaker, 200 mL of dichlorobenzene, 20 g of KH570, and 20 g of nano-SiO_2 were uniformly dispersed under magnetic stirring. The mixture was heated to 90 °C and maintained at this temperature for 10 h. The product was then washed several times with toluene and ethanol, followed by centrifugation, filtration, and drying to obtain the silane-coupling agent-modified nano-SiO_2 (output 22.8 g). In the second stage, 10 g of HTMA, 10 g of EP, and 5 g of KH570-SiO_2 were dispersed in 100 mL of deionized water and heated to 60 °C, maintaining this temperature for 3 h. Upon completion of the reaction, the mixture was washed several times with ethanol and dried at 60 °C to yield the final white powder product, referred to as EP-HMTA-SiO_2 (output 13.6 g).

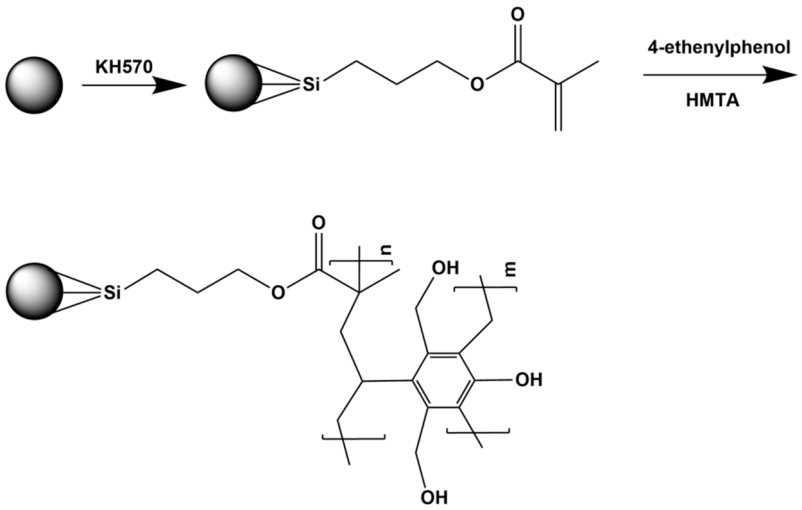


Figure 1. The preparation of EP-HMTA-SiO_2.

2.3. The Characterization of EP-HMTA-SiO_2

The FT-IR measurements were conducted with a NEXUS FT-IR spectrometer (Thermo Nicolet Corporation). The KBr pellets prepared by pressing mixtures of 1 mg of powder sample and 100 mg of KBr were scanned between 4000 and 400 cm^{-1} range with spectral resolution of 4 cm^{-1}. The SEM measurements were performed using a Sigma 300 instrument. The TGA was performed on a Versa Therm HM thermogravimetric analyzer. The sample dispersion used for the particle size distribution measurement was prepared using ultrasound dispersion by a multi-angle granularity analyzer (NanoBrook Omni, Brookhaven Instruments).

2.4. Interface Tension Measurements

The interfacial tension was measured using a TX-500C type interfacial tensiometer. The oil phase used was crude oil from the target oil field (dehydrated and degassed), with a testing temperature of 60 °C and a rotation speed of 8000 r/min. The interfacial tension was calculated using Formula (1).

$$\gamma = \frac{\nabla\rho\omega^2 r^3}{4}\left(\frac{l}{d} \geq 4\right) \quad (1)$$

In this formula, $\nabla\rho$ represents the density difference between the oil and water phases ($kg{\cdot}m^{-3}$). ω is the angular velocity ($rad{\cdot}s^{-1}$), r is the radius of the short axis of oil droplet (m), l is the length of the centrifuge tube (m), and d is the diameter of the centrifuge tube (m).

2.5. Contact Angle Measurements

Clean glass slides were separately immersed in water for 24 h, followed by drying at 60 °C for 24 h to make its surface hydrophobic to reduce the impact of surface stains. The EP-HMTA-SiO_2 solution with different mass fraction was added to the surface of the slide, and the contact angle between the test solution, and the slide was measured with SPCA-X3 contact angle goniometer.

2.6. Viscosity Measurements

A series of EP-HMTA-SiO_2 solutions with varying mass fractions were prepared using simulated formation water as the base fluid. The viscosity of the solutions at different temperatures was measured using a DVPL-type Brookfield viscometer, with a shear rate of 6 rad/s.

2.7. Oil Recovery Efficiency Measurements

The recovery efficiency of 0.4 wt% of SiO_2 and EP-HMTA-SiO_2 was evaluated using sand pack with permeabilities of 200×10^{-3} μm^2 and 20×10^{-3} μm^2. The displacement experiments were conducted at a temperature of 60 °C and an injection rate of 0.5 $mL{\cdot}min^{-1}$.

3. Results and Discussion

3.1. The Characterization of EP-HMTA-SiO_2

3.1.1. The FTIR of EP-HMTA-SiO_2

The infrared (IR) spectra of SiO_2 and EP-HMTA-SiO_2 are presented in Figure 2. A prominent peak at 3460 cm^{-1} is observed, indicative of hydroxyl groups, either as surface hydroxyls or as constituents of the functionalized polymer matrix. In addition, several characteristic peaks are observed at 474.41 cm^{-1}, 811.90 cm^{-1}, and 1101.17 cm^{-1}, corresponding to the bending vibration, symmetric stretching vibration, and asymmetric stretching vibration of Si-O-Si, respectively [21]. These bands are typical for silica-based materials and confirm the retention of the silica backbone structure. Notably, these functional groups, which are associated with the silica network, are present in both the unmodified SiO_2 and the modified EP-HMTA-SiO_2, suggesting that the polymer modification process does not alter the fundamental Si-O-Si framework. This is important as it demonstrates that the core structure of SiO_2 remains intact despite the grafting of organic polymer chains. A key feature in the IR spectrum of the modified SiO_2 material is the peak at 1640.25 cm^{-1}, which corresponds to the characteristic vibration of the phenolic group [22]. This peak is a clear indication of the successful grafting of vinylphenol onto the surface of SiO_2, confirming that the polymerization of 4-vinylphenol onto the SiO_2 surface was successful. The presence of this phenolic group provides strong evidence for the successful modification of SiO_2 with EP-HMTA, thereby supporting the synthesis of the modified EP-HMTA-SiO_2 material.

These IR spectroscopic results not only substantiate the modification process but also underscore the simultaneous retention of the SiO_2 core structure and the successful incorporation of polymeric functionalities, which endow the material with enhanced physicochemical properties tailored for its intended applications.

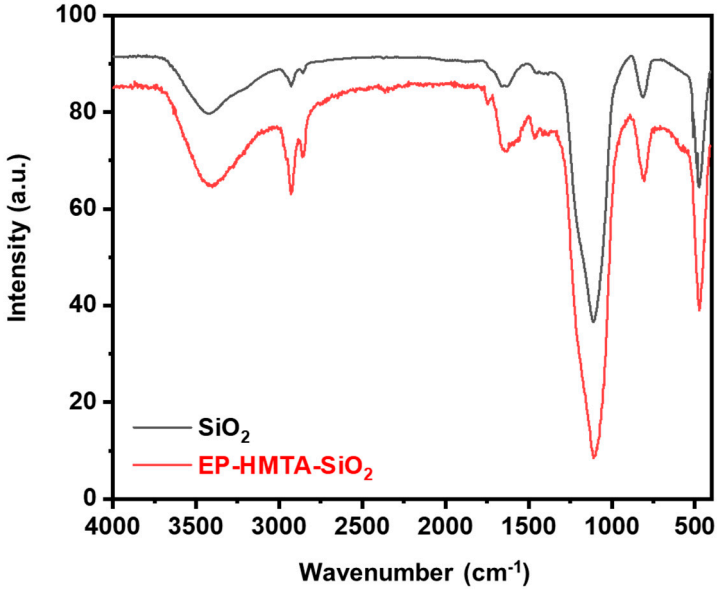


Figure 2. The FTIR curves of SiO_2 and EP-HMTA-SiO_2.

3.1.2. The SEM of EP-HMTA-SiO_2

The SEM images of SiO_2 and EP-HMTA-SiO_2 are shown in Figure 3. As seen in Figure 3a, the surface of the nano-SiO_2 microspheres is smooth with a well-defined spherical morphology, and the particle size is approximately 0.6 μm. After modification with EP and HMTA, the surface becomes rougher, and the spherical morphology is less defined. The particle size appears to have been increased considerably in the modification process, between 1.5 and 5 μm, indicating that the surface has been coated with other materials. This observation further confirms the successful synthesis of EP-HMTA-SiO_2.

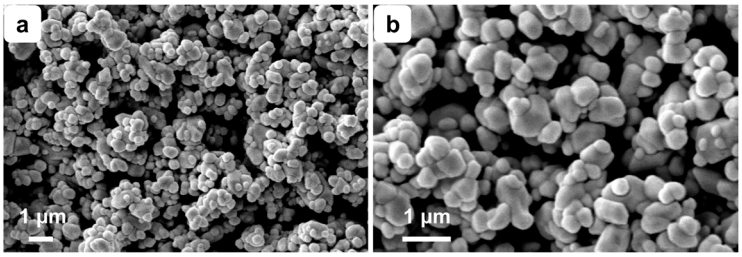


Figure 3. The SEM images of (**a**) SiO_2 and (**b**) EP-HMTA-SiO_2.

3.1.3. The TG of EP-HMTA-SiO_2

The thermogravimetric (TG) curves of SiO_2 and EP-HMTA-SiO_2 are presented in Figure 4, illustrating the thermal stability and decomposition characteristics of both materials. Over the temperature range of 50 °C to 1000 °C, the mass loss rate of SiO_2 nanoparticles is 3.54%, which can be primarily attributed to the evaporation of adsorbed water molecules from the surface of the silica particles [23]. This relatively low mass loss indicates the stability of the SiO_2 framework at higher temperatures. Usually, the melting point of silica is greater than 1500 °C, and the boiling point is greater than 2200 °C

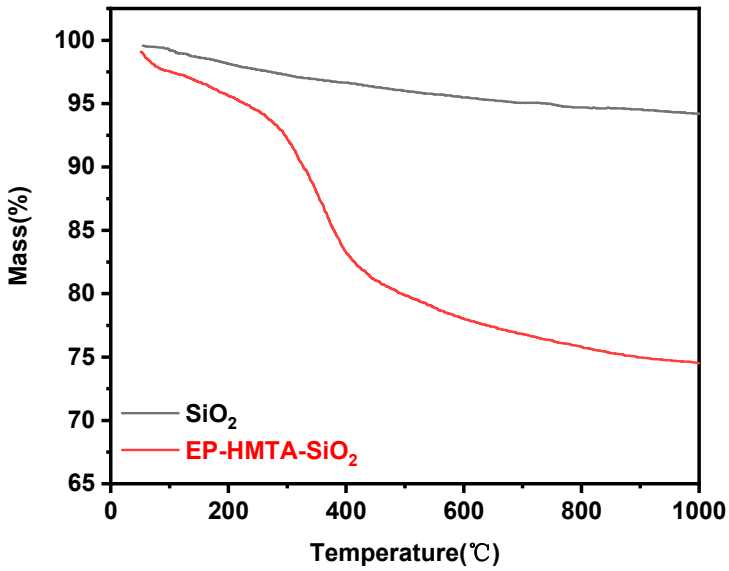


Figure 4. The TG curves of SiO_2 and EP-HMTA-SiO_2. (Nitrogen as the flowing gas).

In contrast, the thermogravimetric (TG) curve of EP-HMTA-SiO_2 exhibits three distinct stages of thermal decomposition, highlighting the complex thermal behavior of the modified material. The first stage, from 50 °C to 120 °C, is associated with the loss of both free and bound water within the material, resulting in a mass loss of 2.74%. This indicates the presence of adsorbed water and hydrated species on the surface or within the structure of EP-HMTA-SiO_2. The second stage, which occurs between 120 °C and 400 °C, corresponds to the degradation of the polymeric molecular chains grafted onto the SiO_2 surface. During this phase, a significant mass loss of 16.36% is observed, suggesting the breakdown of the structure of polymer. This thermal degradation is indicative of the successful grafting of polymer chains, such as EP-HMTA, onto the SiO_2 surface, as the polymer undergoes chain scission and decomposition [24]. Finally, when the temperature exceeds 400 °C, the curve shows a mass loss of 6.36%, which is attributed to the high-temperature decomposition and oxidation of carbonized polymeric residues. This phase involves the combustion or decomposition of the polymeric residues, confirming the presence of organic components in the modified SiO_2 material.

These thermogravimetric findings provide robust evidence for the successful synthesis of EP-HMTA-SiO_2, confirming the structural integrity of the SiO_2 core and the effective incorporation of polymer chains. Moreover, the observed thermal stability enhancements underscore the potential of this material for applications requiring improved thermal resilience and functional durability.

3.1.4. Particle Size Distribution

The particle size distribution of SiO_2 and EP-HMTA-SiO_2 is shown in Figure 5. The median particle size of nano-SiO_2 is 2.05 μm, which may be attributed to the large specific surface area of SiO_2, leading to significant adsorption energy that promotes particle aggregation and ultimately increases the particle size. In contrast, the median particle size of EP-HMTA-SiO_2 is 34.96 μm, indicating that crosslinking of the polymer on the SiO_2 surface has occurred, resulting in an increase in particle size. The wide particle size distribution enables the plugging material to better match the pores of different sizes so as to realize the effective plugging of high seepage channels and reduce the fingering phenomenon in the process of displacement.

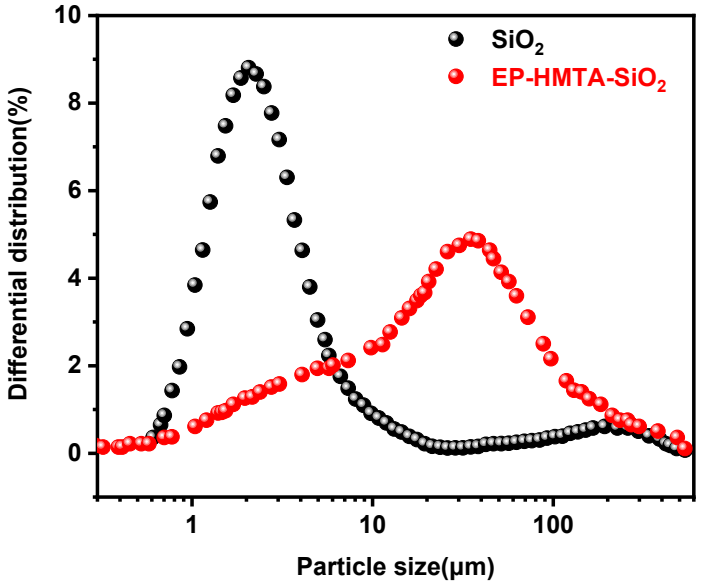


Figure 5. The particle size distribution of SiO_2 and EP-HMTA-SiO_2.

3.2. Effect on Interfacial Tension

Adding modified materials to displacement fluids can reduce surface tension, thereby reducing capillary forces within rock pores. This reduction in capillary forces helps prevent the entrapment of crude oil in the pore spaces of the reservoir, thereby improving the oil recovery rate [25]. As illustrated in Figure 6, the modified EP-HMTA-SiO_2 is particularly effective in lowering the interfacial tension of the solution, consistently maintaining values lower than those observed for unmodified SiO_2. This improvement can be attributed to the ability of polymers to increase the viscosity of the solution, which enhances its ability to reduce surface tension. Moreover, the relationship between EP-HMTA-SiO_2 concentration and interfacial tension reveals an interesting trend.

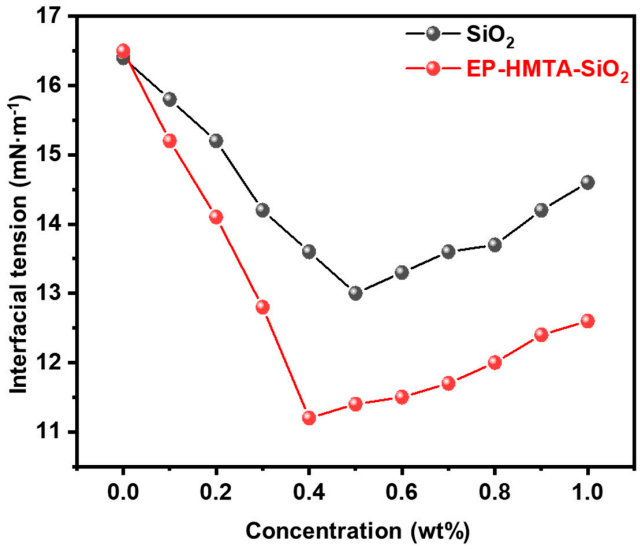


Figure 6. The effect of EP-HMTA-SiO_2 concentration on interfacial tension. (These are aqueous solution concentrations).

As the concentration of EP-HMTA-SiO_2 increases, the interfacial tension initially decreases, reaching a minimum, and then it begins to increase with further concentration. This behavior can be explained by the synergistic interaction between the polymer and inorganic nanoparticles at lower concentrations. At these concentrations, the polymer and

nanoparticles work together to effectively reduce surface tension, likely through mechanisms such as steric hindrance and enhanced molecular interactions at the interface [26,27]. However, at higher concentrations of EP-HMTA-SiO_2, the situation changes. The polymer and nanoparticles begin to form hydrogen bonds, which lead to their adsorption and aggregation at the oil–water interface. This aggregation induces an increase in interfacial tension due to the formation of a denser layer at the interface, which restricts the material's capacity to further reduce surface tension. This concentration-dependent transition in interfacial tension underscores the intricate interplay of molecular interactions that governs the behavior of EP-HMTA-SiO_2 in modifying interfacial properties.

3.3. Effect on Contact Angle

The wettability of rock surfaces plays a crucial role in determining the migration and displacement of crude oil within the pore spaces, which ultimately impacts the efficiency of oil recovery. Materials that alter the wettability of reservoir rocks can significantly influence the flow dynamics of crude oil, and their effects are typically evaluated through contact angle measurements [28]. As shown in Figure 7, the contact angle on hydrophilic surfaces decreases with increasing concentrations of EP-HMTA-SiO_2, initially showing a significant reduction before stabilizing at higher concentrations. Specifically, at a concentration of 0.4 wt% EP-HMTA-SiO_2, the contact angle drops to 32.8°, and subsequent increases in the EP-HMTA-SiO_2 concentration have little effect on further reducing the contact angle. This behavior can be attributed to the high density of hydroxyl groups on the surface of EP-HMTA-SiO_2. These hydroxyl groups are capable of forming strong hydrogen bonds with hydrophilic interfaces, which facilitates better interaction between the polymer and the rock surface. This interaction leads to an improvement in the wettability of the interface, promoting more favorable oil displacement conditions. At lower concentrations, the polymer molecules can effectively adsorb to the rock surface, modifying the wettability and lowering the contact angle. However, once the concentration of EP-HMTA-SiO_2 reaches a certain critical threshold, the adsorption of the material at the oil–water–rock interface reaches saturation. At this point, no further increase in the amount of EP-HMTA-SiO_2 occurs, and the contact angle stabilizes, showing no significant changes despite further increases in concentration. This saturation effect suggests that the wettability modification is primarily governed by the concentration of EP-HMTA-SiO_2 that can be effectively adsorbed at the interface, beyond which the excess material yields negligible effects on the contact angle.

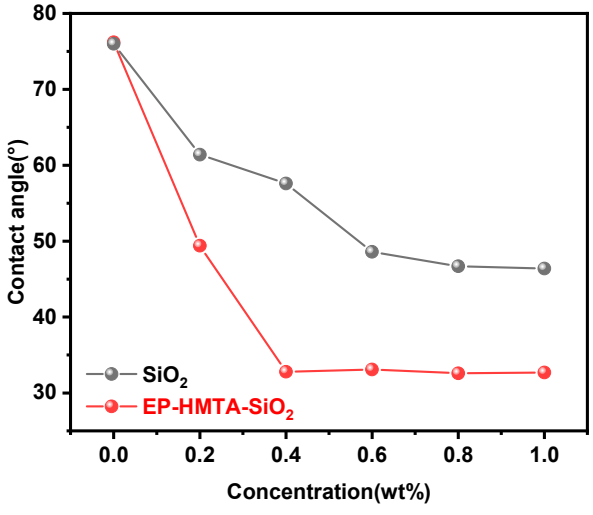


Figure 7. The effect of concentration (EP-HMTA-SiO_2 and SiO_2) on contact angle.

3.4. Evaluation of Viscosity

As the viscosity of the polymer solution increases, the water–oil mobility ratio decreases, which in turn enhances the swept volume and ultimately improves the oil recovery efficiency. This relationship is critical, because a higher viscosity reduces the relative mobility of water, allowing the injected fluid to displace oil more effectively from the pore spaces, thus increasing the overall recovery [29].

As illustrated in Figure 8, under constant temperature conditions, the viscosity of the EP-HMTA-SiO_2 solution increases proportionally with rising EP-HMTA-SiO_2 concentration, demonstrating a strong positive correlation between polymer concentration and solution viscosity. At a fixed concentration of EP-HMTA-SiO_2, the viscosity of the solution shows a slight decreasing trend as temperature increases, although the change remains relatively small. This behavior arises from the fact that the EP-HMTA-SiO_2 polymer contains numerous hydrophilic groups and large molecular side chains, which contribute to significant steric hindrance and molecular entanglement. These factors increase the resistance to flow, thereby enhancing the viscosity of the solution. As the concentration of EP-HMTA-SiO_2 increases, the intermolecular interactions, such as hydrogen bonding and van der Waals forces, become more pronounced, further enhancing the viscosity due to stronger molecular interactions and the physical bulkiness of the polymer chains. However, with an increase in temperature, some of the polymer side chains undergo thermal degradation or relaxation, leading to a reduction in the overall viscosity. This temperature-induced decrease in viscosity is expected, as higher temperatures typically reduce the rigidity and entanglement of polymer chains. Nonetheless, due to the presence of abundant large molecular side chains and substantial steric hindrance effects, the viscosity of the EP-HMTA-SiO_2 solution exhibits only a marginal decrease with temperature. The persistent steric effects and the considerable molecular size of the polymer alleviate the impact of temperature on viscosity, ensuring that the solution maintains a sufficiently high viscosity for effective oil displacement.

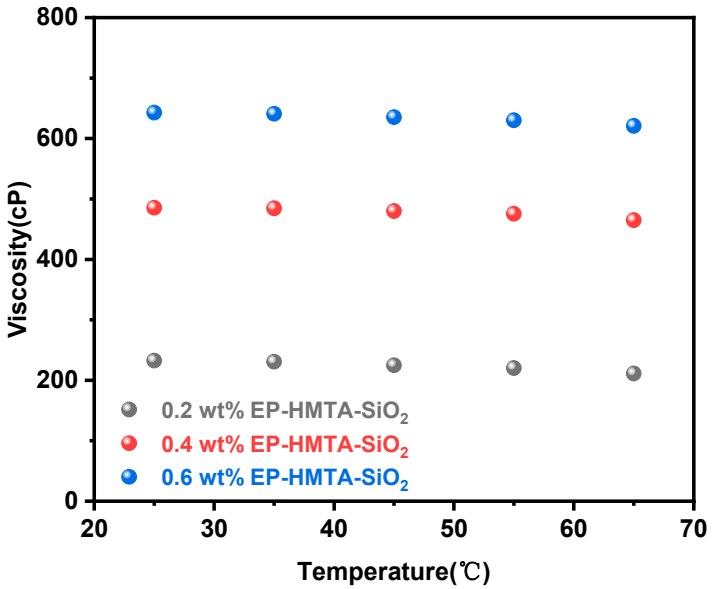


Figure 8. The effect of EP-HMTA-SiO_2 concentration on viscosity.

3.5. Evaluation of Oil Recovery Efficiency

The results of the displacement experiments are presented in Figure 9, which illustrate the impact of injection volume on oil recovery efficiency. As the injection volume increased, the recovery rates for water flooding were found to be 40.2% and 33.8% for medium- and

low-permeability cores, respectively. However, after the injection of 0.4 wt% SiO_2 and EP-HMTA-SiO_2 solutions, the recovery rates in the medium-permeability cores showed significant improvements of 9.1% and 16.4%, respectively. Notably, both recovery rates for the modified SiO_2 solutions were higher than those observed in low-permeability reservoirs, which highlights the enhanced recovery potential of these materials. This observed increase in recovery efficiency can be attributed to several factors. First, medium-permeability cores generally have larger pore throat sizes compared to low-permeability cores, which facilitates the displacement of crude oil by the injected solutions. The larger pores and throats allow more particles to penetrate and mobilize trapped oil, contributing to the increased recovery. Additionally, the higher recovery rates in the medium-permeability cores can also be explained by the ability of the modified SiO_2 (especially EP-HMTA-SiO_2) to effectively alter the wettability of the rock surfaces, reduce interfacial tension, and increase solution viscosity, all of which improve oil displacement efficiency. Conversely, in low-permeability reservoirs, smaller pore sizes and stronger capillary forces impede oil displacement, making it more challenging for the injected solutions to effectively sweep the oil out. While the injection of SiO_2 and EP-HMTA-SiO_2 yields measurable recovery improvements in low-permeability cores, the magnitude of enhancement remains less pronounced, constrained by these inherent reservoir characteristics.

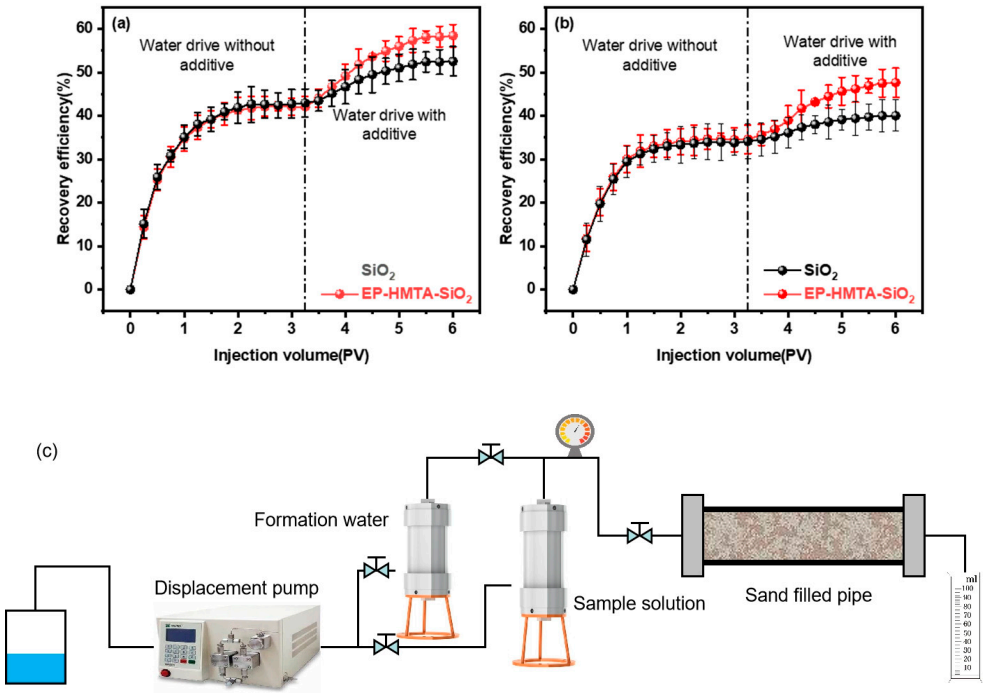


Figure 9. Evaluation of oil recovery: (**a**) medium-permeability cores, (**b**) low-permeability cores, (**c**) diagram of simulation testing process.

Overall, the enhanced recovery observed in both medium- and low-permeability cores reinforces the effectiveness of SiO_2 and EP-HMTA-SiO_2 as promising additives for improving oil recovery, particularly in medium-permeability reservoirs, where particle displacement and interfacial property modifications exert a more pronounced impact.

3.6. Mechanism Investigation

The polymer coating on the surface of SiO_2 is characterized by a high density of large molecular side chains and hydroxyl groups, which endow the material with several distinct properties. These structural features contribute to exceptional thermal stability and significantly enhanced viscosity, enabling the material to maintain a consistently high

solution viscosity across a broad temperature range. This characteristic is particularly beneficial in reducing interfacial tension between the oil and water phases, as a lower interfacial tension promotes more efficient fluid displacement (Figure 10). Moreover, the elevated viscosity of the solution not only reduces the water–oil mobility ratio but also helps to enhance the swept volume within the reservoir, thereby improving the overall oil recovery efficiency [30].

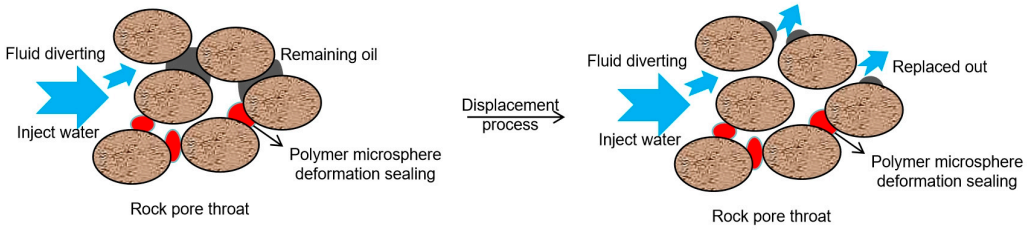


Figure 10. Mechanism of enhancing oil recovery efficiency.

In addition to these effects, the abundant hydroxyl groups on the polymer surface play a crucial role in optimizing the wettability of the reservoir rock. By enhancing the hydrophilicity of the surface, the polymer strengthens the interaction between the oil and the rock matrix, thereby facilitating more efficient migration of crude oil within the pore spaces [31]. This, in turn, reduces oil trapping and enhances the overall displacement efficiency. The combined effect of these mechanisms contributes to a significant increase in recovery rates. This comprehensive interplay between viscosity control, interfacial tension reduction, and wettability modification highlights the potential of EP-HMTA-SiO_2 as an effective agent for improving enhanced oil recovery processes.

4. Conclusions

In this study, considering the temperature resistance issues faced by polymers and the insufficient adaptability of silica materials, EP, and HMTA were successfully grafted onto the surface of nanosilica through a two-step reaction process, resulting in the formation of EP-HMTA-SiO_2. Compared to unmodified SiO_2, the modified material exhibits large molecular side chains and a high density of hydroxyl groups. These modifications introduce significant steric hindrance, which enhances the thermal stability and viscosity of material. The increased viscosity is advantageous for reducing interfacial tension and contact angle, which are critical factors in the enhanced oil recovery process. Specifically, the reduction in interfacial tension helps to decrease the capillary forces in rock pores, facilitating the displacement of crude oil. Additionally, the lower contact angle improves the wettability of the rock surfaces, promoting better oil mobility within the reservoir. The increase in polymer solution viscosity further contributes to improved recovery by reducing the water–oil mobility ratio, thereby enhancing the swept volume and overall displacement efficiency. Performance evaluations demonstrated that the injection of 0.4 wt% EP-HMTA-SiO_2 resulted in recovery rate improvements of 16.4% and 13.2% in medium- and low-permeability cores, respectively. This improvement can be attributed to the combined effects of enhanced viscosity and optimized wettability. The results indicate that EP-HMTA-SiO_2 is effective in improving recovery efficiency, particularly in medium- and low-permeability reservoirs. Overall, the modified EP-HMTA-SiO_2 exhibits substantial potential for enhanced oil recovery. Its ability to increase solution viscosity and fine-tune the wettability of reservoir rocks positions it as a promising candidate for boosting recovery efficiency in challenging reservoirs, where traditional methods often prove less effective.

Author Contributions: W.Z., Conceptualization, Investigation, Writing-original draft; Y.S., Methodology, Investigation, Writing—original draft; X.M., Data curation, Writing—original draft; R.D., Methodology, Investigation, Writing—review and editing. All authors have read and agreed to the published version of the manuscript.

Funding: The authors acknowledge the financial support for the National Key R&D Program of China (2019YFA0708700).

Data Availability Statement: No new data were created or analyzed in this study.

Conflicts of Interest: The authors declare no conflicts of interest.

References

1. Kakati, A.; Bera, A.; Al-Yaseri, A. A review on advanced nanoparticle-induced polymer flooding for enhanced oil recovery. *Chem. Eng. Sci.* **2022**, *262*, 117994. [CrossRef]
2. Tavakkoli, O.; Kamyab, H.; Shariati, M.; Mohamed, A.M.; Junin, R. Effect of nanoparticles on the performance of polymer/surfactant flooding for enhanced oil recovery: A review. *Fuel* **2022**, *312*, 122867. [CrossRef]
3. Saw, R.K.; Singh, A.; Maurya, N.K.; Mandal, A. A mechanistic study of low salinity water-based nanoparticle-polymer complex fluid for improved oil recovery in sandstone reservoirs. *Colloids Surf. A Physicochem. Eng. Asp.* **2023**, *666*, 131308. [CrossRef]
4. Amiri, M.; Fatemi, M.; Delijani, E.B. Effect of brine salinity and hydrolyzed polyacrylamide concentration on the Oil/Brine and Brine/Rock Interactions: Implications on enhanced oil recovery by hybrid low salinity polymer flooding in sandstones. *Fuel* **2022**, *324*, 124630. [CrossRef]
5. Ghamarpoor, R.; Jamshidi, M.; Alhaeehm, Z. Synthesis of Hybrid/Superhydrophobic Coupling Agent Grafted Nano SiO_2 and Its Use in Fabrication of Rubber Nanocomposite with Outstanding Oil/Water Separation Capability. *Results Eng.* **2024**, *22*, 102270. [CrossRef]
6. Liu, J.; Almakimi, A.; Wei, M.; Bai, B.; Hussein, I.A. A comprehensive review of experimental evaluation methods and results of polymer micro/nanogels for enhanced oil recovery and reduced water production. *Fuel* **2022**, *324*, 124664. [CrossRef]
7. Koolivand, M.; Shokouhi, M.; Esfandyari, M.; Sadeghi, M. A review of fabrication methods for biodegradable pH-Responsive nanocomposite microgels and their performance in enhanced oil recovery. *S. Afr. J. Chem. Eng.* **2024**, *50*, 340–352. [CrossRef]
8. Liu, Y.; Zhou, L.; Wan, X.; Tang, Y.; Liu, Q.; Li, W.; Liao, J. Synthesis and characterization of a temperature sensitive microcapsule gelling agent for high-temperature acid release. *ACS Omega* **2024**, *9*, 20849–20858. [CrossRef]
9. Du, W.; Wang, T.; Xie, Z.; Xia, L.; Lu, J.; Li, P. Superhydrophobic SiO_2 microspheres of a porous dehydroabietic-acid-based homopolymer for oil-water separation. *Sep. Purif. Technol.* **2024**, *340*, 126838. [CrossRef]
10. Pal, N.; Manadal, A. Compositional simulation model and history-matching analysis of surfactant-polymer-nanoparticle (SPN) nanoemulsion assisted enhanced oil recovery. *J. Taiwan Inst. Chem. Eng.* **2021**, *122*, 1–13. [CrossRef]
11. Gazem, A.; Patel, H.; Sreenivasan, H.; Sahu, C.; Krishna, S. Combined effect of silica nanoparticles and binary surfactants in enhancing oil recovery: An experimental investigation. *Colloids Surf. A Physicochem. Eng. Asp.* **2024**, *702*, 134980. [CrossRef]
12. Nyah, F.; Ridzuan, N.; Nwaichi, P.I.; Umunnawuike, C.; Agi, A. Comprehensive review on the role of salinity on oil recovery mechanisms during chemical flooding. *J. Mol. Liq.* **2024**, *415*, 126308. [CrossRef]
13. Hou, K.; Wu, H.; Xu, G.; Li, G.; Luan, T.; Chang, J.; Cheng, T.; Song, Z.; Hou, J. A CO_2-responsive Janus SiO_2 nanofluid: Integration of enhanced oil recovery and demulsification. *J. Mol. Liq.* **2024**, *412*, 125832. [CrossRef]
14. Pal, N.; Mandal, A. Enhanced oil recovery performance of gemini surfactant-stabilized nanoemulsions functionalized with partially hydrolyzed polymer/silica nanoparticles. *Chem. Eng. Sci.* **2020**, *226*, 115887. [CrossRef]
15. Manshad, A.K.; Ali, J.A.; Haghighi, O.M.; Sajadi, S.M.; Keshavarz, A. Oil recovery aspects of ZnO/SiO_2 nano-clay in carbonate reservoir. *Fuel* **2022**, *307*, 121927. [CrossRef]
16. Tliba, L.; Sagala, F.; Hethnawi, A.; Glover, P.W.; Menzel, R.; Hassanpour, A. Surface-modified silica nanoparticles for enhanced oil recovery in sandstone cores. *J. Mol. Liq.* **2024**, *413*, 125815. [CrossRef]
17. Pal, N.; Mandal, A. Oil recovery mechanisms of Pickering nanoemulsions stabilized by surfactant-polymer-nanoparticle assemblies: A versatile surface energies' approach. *Fuel* **2020**, *276*, 118138. [CrossRef]
18. Xia, H.; Wang, D.; Liu, Z.; Yang, Q. Study on the mechanism of polymer solution with viscoelastic behavior increasing microscopic oil displacement efficiency. *Acta Pet. Sin.* **2001**, *22*, 60–65.
19. Lei, T.; Wang, Y.; Zhang, H.; Cao, J.; Xiao, C.; Ding, M.; Chen, W.; Chen, M.; Zhang, Z. Preparation and performance evaluation of a branched functional polymer for heavy oil recovery. *J. Mol. Liq.* **2022**, *363*, 119808. [CrossRef]
20. Cheng, Y.; Jing, D.U.; Luo, W. Synthesis and properties of oil displacement agent nanosilica grafted poly-acrylmide/2-acrylamido-2-methyl-l-propanesulfonic acid sodium. *Chem. Res.* **2017**, *28*, 230–235.

21. Zhong, H.; Gao, X.; Zhang, X.; Qiu, Z.; Zhao, C.; Zhang, X.; Jin, J. Improving the shale stability with nano-silica grafted with hyperbranched polyethyleneimine in water-based drilling fluid. *J. Nat. Gas Sci. Eng.* **2020**, *83*, 103624. [CrossRef]
22. Li, J.; Wen, M.; Yang, J.; Liu, Y.; Jiang, Z.; Chen, J. Synthesis and analysis of magnetic nanoparticles within foam matrix for foam drainage gas production. *Geoenergy Sci. Eng.* **2024**, *238*, 212887. [CrossRef]
23. Wang, L.; Li, J.; Wang, Y.; Cheng, S.; Ma, C. Effects of SiO_2-coated CNTs on the directional formation of SiC whiskers and improvement in the ablative resistance of polymer-matrix composites. *Compos. Sci. Technol.* **2024**, *258*, 110904. [CrossRef]
24. Safronova, E.Y.; Yurova, P.A.; Ashrafi, A.M.; Chernyak, A.V.; Khoroshilov, A.V.; Yaroslavtsev, A.B. The effect of ultrasonication of polymer solutions on the performance of hybrid perfluorinated sulfonic acid membranes with SiO_2 nanoparticles. *React. Funct. Polym.* **2021**, *165*, 104959. [CrossRef]
25. Li, J.; Wen, M.; Jiang, Z.; Gao, S.; Xiao, X.; Xiang, C.; Tao, J. Formulation and characterization of surfactants with antibacterial and corrosion-inhibiting properties for enhancing shale gas drainage and production. *Sci. Rep.* **2025**, *15*, 2376. [CrossRef] [PubMed]
26. Tang, W.; Zou, C.; Liang, H.; Da, C.; Zhao, Z. The comparison of interface properties on crude oil-water and rheological behavior of four polymeric nanofluids (nano-SiO_2, nano-CaO, GO and CNT) in carbonates for enhanced oil recovery. *J. Pet. Sci. Eng.* **2022**, *214*, 110458. [CrossRef]
27. Yu, X.; Ji, R.; Li, Q.; Yong, S.; Yang, H.; Su, G. Core-shell polymer microsphere PSN@SiO_2 based on "dry water microreactor" for enhanced oil recovery and its properties. *Geoenergy Sci. Eng.* **2024**, *239*, 212972. [CrossRef]
28. Hou, C.; Fan, Z.; Yang, J. Construction of super hydrophobic paper by modified nano-SiO_2 hybrid medium fluoro-epoxy polymer and its properties. *Prog. Org. Coat.* **2024**, *187*, 10818. [CrossRef]
29. Li, J.; Wen, M.; Jiang, Z.; Xian, L.; Liu, J.; Chen, J. Development and characterization of a surfactant responsive to redox conditions for gas recovery in foam drainage. *Sci. Rep.* **2025**, *15*, 511. [CrossRef] [PubMed]
30. Xu, H.; Zhu, Y.; Liu, Y.; Fan, W.; Tang, L.; Chen, T.; Wang, Y.; Yang, F. Temperature-sensitive polymer grafted with nano-SiO_2 improves sealing and inhibition performance of shale water-based drilling fluid. *Colloids Surf. A Physicochem. Eng. Asp.* **2024**, *698*, 134531. [CrossRef]
31. Li, X.; Gao, D.; Liu, M.; Zheng, L.; Li, P.; Lyu, B. Synthesis of amphiphilic Janus SiO_2/styrene butyl acrylate polymer microspheres and their application in oil recovery. *Colloids Surf. A Physicochem. Eng. Asp.* **2023**, *675*, 132076. [CrossRef]

Disclaimer/Publisher's Note: The statements, opinions and data contained in all publications are solely those of the individual author(s) and contributor(s) and not of MDPI and/or the editor(s). MDPI and/or the editor(s) disclaim responsibility for any injury to people or property resulting from any ideas, methods, instructions or products referred to in the content.